A method to replace lightning strike tests by ball impacts in the design process of lightweight composite aircraft panels

F. Soulas, Christine Espinosa, Frederic Lachaud, S. Guinard, Bruno Lepetit, I. Revel, Y. Duval

A method to replace lightning strike tests by ball impacts in the design process of lightweight composite aircraft panels

F. Soulas[a,b,1], C. Espinosa[a,1,*], F. Lachaud[a,1], S. Guinard[b], B. Lepetit[b], I. Revel[b], Y. Duval[b]

[a] Institut Clément Ader (ICA), Université de Toulouse, CNRS-INSA-ISAE-Mines Albi-UPS, 3 Rue Caroline Aigle, Toulouse Cedex 4 31077, France
[b] Airbus Group Innovations, Bât. Campus engineering, BP90112, Blagnac Cedex 31703, France

Keywords:
Lightning
Impact
Damage
Carbon fibre reinforced plastics
Numerical simulations

A B S T R A C T

Composite material aircrafts are protected against lightning on the basis of complex and expansive lightning strike experimental plans aiming at designing optimal protections. The paper aims at reducing the number of lightning strike tests on protected and painted composite panels. An analytical calculation is presented that gives the characteristics of an equivalent mechanical impact configuration based on an assessment of the typical time scale of energy deposit and kinematic behaviour during a lightning strike test. The paper presents our analytical hypotheses and calculations, as well as experimental lighting strikes and mechanical impact settings and results. The method is shown to give an acceptable approximation of both the kinematics and the delamination surface.

1. Introduction and context

Lightning Strikes (LS) are responsible for two major effects on lightweight aeronautical composite structures: direct and indirect. The focus of this study is put on direct effects which mainly concern the structural damage resistance of stroke panels to LS, and the risk of explosion at the rear face in case of fuel casing. For modelling purposes, two points are to be determined: the kind of damage under interest for the structural damage resistance, and the kind of loading that propagates through the composite panel from the protected to the rear face. We are interested here in the final damage state affecting the residual strength.

1.1. Damage in protected composite panels

Lightning material interaction involves several complex phenomena involving, electromagnetic and thermal components as well as probable coupling between them that are not easily measureable and quantifiable. When it impacts metallic materials, lightning generally induces the melting and the cutting of the materials as well as its deflection [1–3]. For Carbon Reinforced Plastic (CFRP) composite materials (typically 1000 times relatively more electrically resistive), lightning induces surface burning and leads to explosion of the laminate and the break up of the fibres around the attachment point on the top face as well as delamination of the composite material through its depth (Fig. 1).

Studies of damage mechanisms under LS on composite materials have been increasing since 2007 [4–11]. Most of them are focused on surface damage inflicted to the lightning strike protection (LSP) layers or to the first plies. Most of the authors have essentially proposed to represent the complex event as resulting from a temperature raise on a small region near the lightning channel attachment point on the material. Due to the extremely high temperature reached and the complex events taking place in LSP layers, phenomenological or computational models represent most of the time bare plates without LSP. But in fact airplanes are always protected. The protection has to absorb the LS energy and to limit the mechanical and thermal transfer in the laminate. It also has to be a good electrical conductor to evacuate the received current and its associated energy away from the lightning strike area. Most common used protections are Expanded Metal Foil (EMF) or Solid Metal Foils (SMF), but conductive paints as well as metallized carbon fibres have also been tested [8]. Unfortunately, these protections have to cover the whole structure and it results in an additional weight that reduces the gain made up by using composite materials. Moreover the systematic coating of these protections with paint decreases the benefits of the protection [12–16]. Such dielectric layers on top of the LSP ones tend to confine the loading and to increase the average size of the resultant damage in composite component [17]. It is then

* Corresponding author.
E-mail addresses: christine.espinosa@isae-supaero.fr (C. Espinosa), frederic.lachaud@isae-supaero.fr, floriane.soulas@gmail.com (F. Lachaud), stephane.guinard@airbus.com (S. Guinard), bruno.lepetit@irsamc.ups-tlse.fr (B. Lepetit), ivan.revel@airbus.com (I. Revel), yohann.duval@airbus.com (Y. Duval).
[1] www.institut-clement-ader.fr.

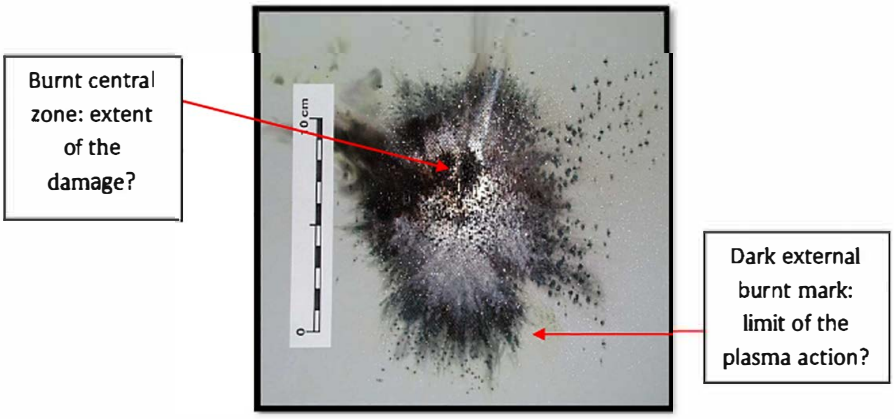

Fig. 1. Visible damage due to lightning impact on a protected composite plate.

necessary to take into account the whole LSP behaviour including paint to model the lightning strike loading.

1.2. Loading transfer from top face to rear face

LSP layers are nowadays designed with help of complex numeri cal simulations and lightning strike tests. Regarding composite pan els, the so called 'components A and D' are known to be the more detrimental regarding the extent of damage produced in the core of the composite samples since they deliver extremely high electrical current (resp. up to 200 kA or 100 kA) in a very short period of time (less than 500 µs, see Fig. 2). Even though the surface is bumed, the core damage is responsible of a higher drop in the residual mechani cal strength and can event create a sparkle or a high temperature at the rear face which can be dramatic at the vicinity of gas tanks. Fol lowing the plane zoning, the D waveform is considered here as the worst case regarding the structural damage and the risk of perfora tion. The physics of damage induced in multi layered thin panels by very rapid loadings including shocks is very complex [18,19]. It this study, it is not intended to model the damage process, but only the final state.

In order to generate the desired current component in lightning tests, High Current Generators (HCG) are used. For the present study, the lightning tests were conducted using the Electromagnetic Means for Aerospace (EMMA) platform at the DGA Techniques Aéronautiques (DGA Ta) in Toulouse (Fig. 3.a).

1.3. Lightning strike models

Several existing models focus on a description of the lightning arc with plasma physics and estimate as a result the extent of damage from matter erosion considerations [12,18 22]. The structure is lim ited to an idealized and simplified boundary of the complex events that are finely represented in the electrical arc. By doing so, they

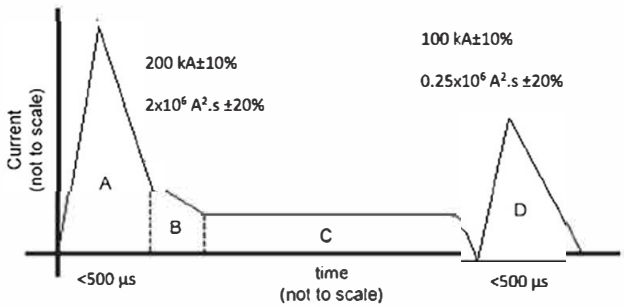

Fig. 2. Standard lightning strike current delivery used in aerospace industry [8].

mainly focus on extensive and visible damage occurring on the first ply and the protection and paint layers when they are considered. However, the most detrimental damages for the composite struc tures are the ones occurring in the bulk of the laminate which, most of the time, are not visible from the outer surfaces after the lightning strike. Such damage as delamination and fibre failure belittle the material mechanical properties sometimes up to complete failure. There is growing evidence that, at least for the impulse A or D com ponents, mechanical phenomena are responsible of core damage. But despite the extensive literature that already exists regarding the impact damage on composite materials due to foreign objects [23 26], only few studies have been published on the mechanical damage due to lightning strike.

The first ones focused on residual strength and structural perfor mance of lightning strike CFRP [16,27 30]. Featherston et al. devel oped a method to assess the shock effect [27]. They tried to predict the peak overpressure forces produced by the shockwave by com paring numerical displacement and velocity of the impacted mate rial with the experimental results. Their work focused on the deflection of aluminium panels and did not take into account the damage resulting from the lightning strike, but it provides interest ing methodology. Hirano et al. [6] investigated the mechanical dam age observed after a lightning strike in order to categorise and understand them. Their study revealed the different types of damage commonly observed in composite laminate after a lightning strike, which are of mechanical origin, mainly cracks in the matrix resin, fibre breakage, and delamination. This damage was found to be dependent on the electrical and thermal properties of the laminate. Other works focus on the impulse waveform of lightning strikes and their effects. Mechanical momentum induced on samples by light ning strikes has been measured, and thermo mechanical models have been proposed to account for the observed damages [31 33]. The thermal model of LS induced damage therefore needs to be sup plemented by mechanical concepts to provide a valuable under standing of the physical damage processes. Haigh et al. [34] made a first step in this direction by focusing on mechanical effects within the material and more particularly on the mechanical impulse (i.e the force transferred by the electrical arc and integrated over time). The mechanical impulse is then extracted from deflection measure ments and compared with traditional mechanical impacts. However, they could still make no clear correlation between mechanical impulse measurements and observed mechanical damage. Gineste et al. [26] pursued the work of Haigh by working on deflection meas urements during lightning strike tests at different location on the impacted material, and developed a thermo mechanical model to describe damage in the material. Karch et al. [35] also worked on lightning current pulse responsible for non thermal damage on pro tected CFRP structures. They focused on the magnetic forces, on the

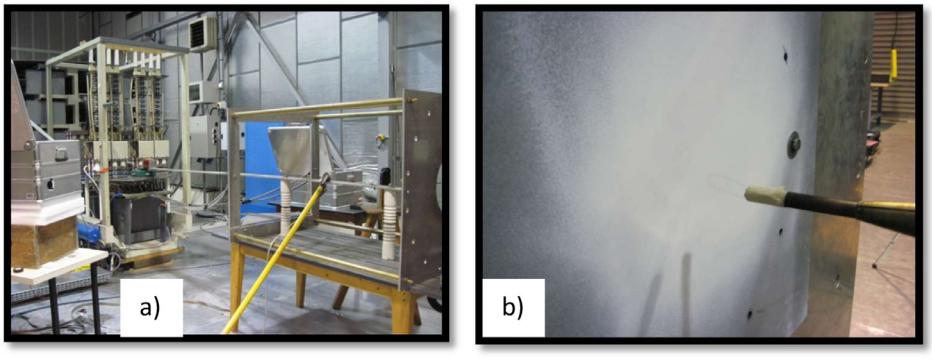

Fig. 3. Lightning generator (a) and electrode for current delivery on test samples (b).

shock waves due to supersonic channel expansion, and on the shock waves due to near surface explosions related to the plasma channel expansion over time and to the size of the arc root radius as initiated in [26]. They demonstrate in particular the small actual contribution of the magnetic forces. Feraboli and Kawakami [17] are the first to compare damage from lightning strikes with traditional low velocity mechanical impact. Their equivalence criterion is the transferred energy in the material, comparing the intensity of the electric arc current with the energy transmitted with mechanical impacts. They showed by using non destructive ultrasonic testing that the mechanical impacts provided larger damage than equivalent light ning strike but that the damages obtained were of the same nature. This is a first step toward a simpler representation and understand ing of lightning direct effects. Further steps involve the usage of multi physics simulations [10,36,37] but which for now don't give more insight into experimental procedures that could replace or reduce complex lightning tests.

The present paper proposes a method to reduce the number of lightning tests necessary in the LSP design, and to replace them by Mechanical Impact (MI) tests able to give the same amount of delaminated surfaces in CFRP samples. The first part presents the Lightning Strike (LS) tests and the hypotheses that can be made on the induced damage. The second part presents the analytical method and calculations that are proposed to determine the mass and veloc ity of the projectile for the equivalent impact test. Results of the MI tests and LS tests are presented and compared.

2. Lightning strike tests

Multiple lightning test campaigns have been run by Airbus Group Innovation (AGI) in order to improve the understanding of the con sequences of lightning on thin composite panels and improve the metallic protections design.

2.1. Lightning strike induced damage

It must be noted though that experimental data acquisition is rather complex in the context of lightning tests. Indeed, lightning is a very fast event (pulse component of the current is less than 100 μs) which involves very high temperatures, up to 30,000 K and very high current intensity up to 200 kA. This induces a very high level of noise in all electronic acquisition devices. Lightning strike tests also generate very bright arcs that tend to saturate traditional cameras disposed for event recording. The rapidity (lightning cur rent discharged in less than 100 μs) and extreme conditions of the tests (luminosity of the arc, extreme temperature of the plasma, and electromagnetic pollution) make the implementation of contact instrumentations on the sample rather tricky. Consequently, during these tests, only two kinds of results were obtained.

Firstly, with the help of an interferometric apparatus, the rear face deflection and velocity of the samples have been measured ver sus time. Secondly, post mortem non destructive and destructive analyses were conducted to measure total delamination area and through thickness distributions. Typical surface damage areas essen tially due to thermal effects are shown on Fig. 4: sublimation of the metallic mesh and removal of the paint above the protection as well as burning of the first ply's carbon fibres and epoxy resin.

Ultrasonic C Scan provides information on the size and shape of the damage in the thickness of the material thanks to a 2D projected view of the damage, as shown on Fig. 5. Due to large openings of the delamination, it is not enough to use C Scan to locate them with high precision in the depth and cuts are necessary to complete the analysis. But still the figure illustrates the large differences between delamination extents because of paint.

This figure presents three different distributions of damage after lightning tests following the same D waveform current delivery (Eq. 1, Fig. 7). Samples (a) (b) and (c) are all protected with Expanded Copper Foils of 195 g/m^2 (ECF195) and respectively covered by paint layers of 200 (a), 700 (b) and 160 (c) μm thickness. All the samples are quasi isotropic [45/0/ 45/90]s UD CFRP epoxy resin composite panels (total thickness 1.45 mm). The ultrasonic analysis is per formed from the rear face of the samples, which is the face opposite to the lightning strike attachment area.

These observations led us to separate two different kinds of dam age found in struck samples. Surface damages seem to be entirely due to thermal and electric effects of the arc root and the current flowing on the top layers of the samples [11]. Microscope

Fig. 4. Typical observable damage after D waveform LS test on a CFRP target.

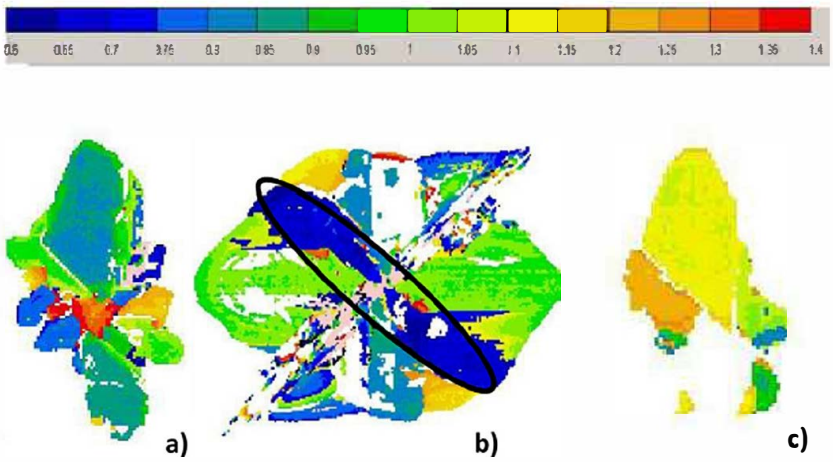

Fig. 5. Ultrasonic C-Scans after lightning strikes with different thicknesses of paint.

observations of the core damage show no evidence of thermal dam age but rather classical mechanical ones similar to damage observed in low velocity impacts [38]: fibre/resin debonding, transverse crack, fibre rupture and ply delamination (see Fig. 6).

2.2. Link between damage and loading

Four 450 × 450 mm^2 square samples clamped on a circle of diam eter Φ370 mm using 12 equally spaced bolts were tested. T700/M21 carbon epoxy plates with [45/0/ 45/90]s layup were used. Samples differ by the type of Expanded Copper Foil (ECF) metallic protection (ECF 73 g/m^2 or ECF 195 g/m^2) and the paint thickness above the protection (No Paint or 200 µm paint, see Table 1).

The current delivered follows a double exponential curve in time (Fig. 7) to reproduce a D waveform, following the certification requirements [39,40].

$$I(t) \quad I_0\left(e^{-\alpha t} \quad e^{-\beta t}\right) \text{ where } I_0 \quad 6.58 \cdot 10^6 \text{A}; \alpha \quad 50000 \text{s}^{-1}; \beta \quad 52000 \text{s}^{-1} \qquad (1)$$

For each test, velocity and displacement (integration of the veloc ity) are measured at the centre of the plate at the opposite face of the lightning strike, using a VISAR (Velocity Interferometer System for Any Reflector). Fig. 8 shows displacement and speed versus time, measured by the VISAR for the samples described in Table 1.

In order to characterise the behaviour of each sample for compar ison, we define four characteristics time (Fig. 8):

'*Short times*': 0 µs to about 50 µs (depends on each test), time interval to reach the maximum value of the velocity at the rear face centre;

Table 1
Presentation of the lightning campaign cases.

Samples #	Surface state
1	NoECF-NoP
2	ECF195-NoP
3	ECF195-P200
4	ECF73-P200

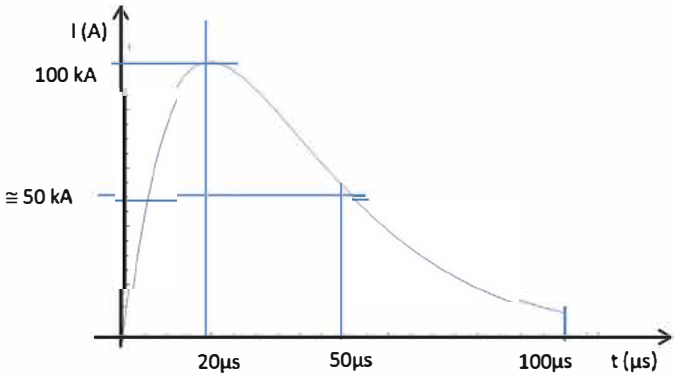

Fig. 7. Idealized current distribution in time.

'*Strike times*': about 50 µs to 100 µs (depends on each test), time interval between maximum value of the velocity and tis mini mum value before the global vibration;
'*Stabilization times*': about 100 µs to 500 µs; time defined by a "plateau" shape of the displacement curves;

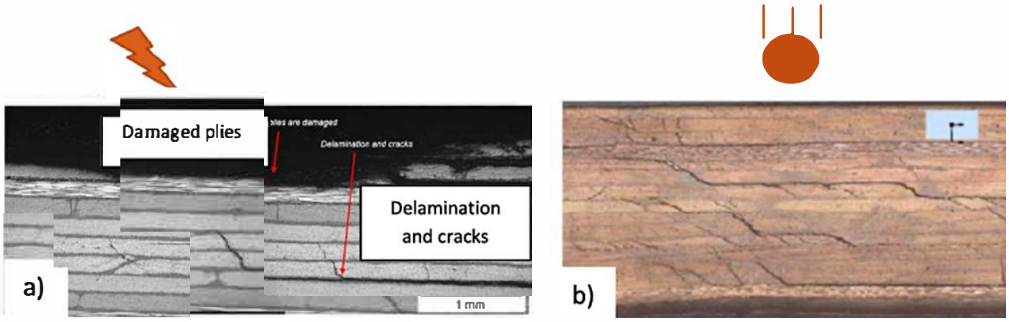

Electrical apparatus (normalized current) Mechanical apparatus (canon and drop tower tests)

Fig. 6. Zoom on micro cuts: difference between thermally damage plies (on the top) and core damage in the thickness similar to mechanical impact induced damage.

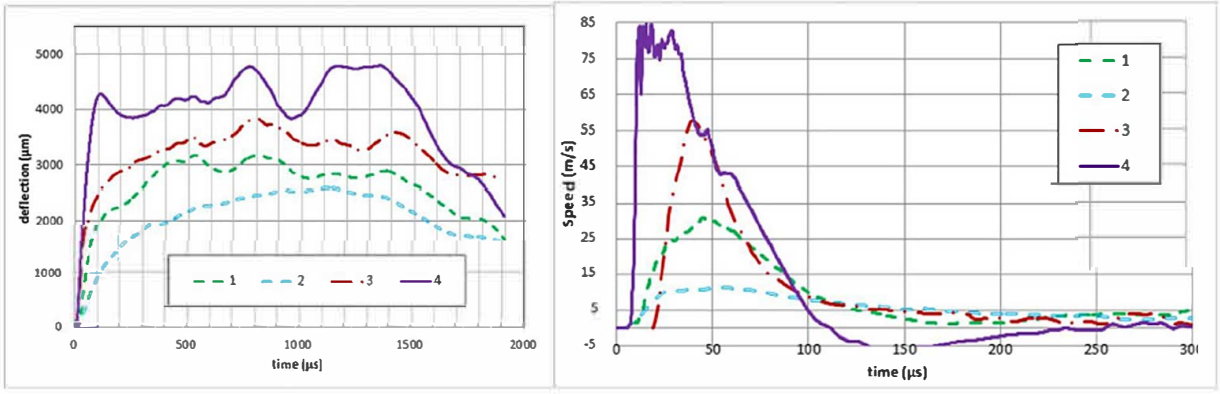

Fig. 8. (a) Deflection and (b) Velocities versus time of the central point at the rear side of the sample subjected to a D waveform lightning strike.

'*Large times*': over 500 µs, peak shock is passed and other phenomena arise like vibrations of the plate.

It is suspected that, as for other fast loadings (impacts, blast e.g.), damages are essentially caused during the period of time in which the mechanical loading is increasing as a consequence of the current energy delivery. This period is called 'short times' here. The loading rates that are responsible of the damage final state in the depth of the sample are faster than the acoustic sound speed, thus lateral boundaries don't influence local damages during this loading phase.

3. Analytical approach

The aim of the present analysis is to define mechanical impact test conditions, which provide speed and deflection at the centre of the rear face as close as possible to the ones measured in the lightning tests. A mechanical impact is defined here by a projectile of a given mass hitting a sample at a given speed, such a projectile is thus to be defined. As a preliminary approach, it is assumed that projectiles are spherical, made out of steel, do not deform, and hit the target normally. Thus, mechanical impacts are fully determined by radius r (thus mass) and velocity v of the projectile. The strategy is to find r and v for a given deflection by solving an inverse problem setting the equivalence of the energy deposit and absorption. To solve this inverse problem, the sudden character of surface explosions is used to estimate the delivered strike impulse. The analytical formulation of the deflection of an infinite plate subjected to a mechanical pressure is then used.

Calculations are made at large times (about 300 μs) which are long enough to authorise considering that the pressure has been fully delivered, and short enough to emphasize that the plate is free of boundary. The Green's function gives the deflection at time t and radius $r = \sqrt{[(x^2 + y^2)]}$ for a Dirac delta function impulse applied at time $t = 0$ at the centre $r = 0$ of an infinite plate ([37], p. 124):

$$G(r,t) \quad \frac{1}{4\pi\sqrt{\mu D}}\left(\frac{\pi}{2}\ Y(t)Si\left(\frac{r^2}{4\sqrt{\frac{D}{\rho h}}t}\right)\right) \tag{2}$$

Where μ is the surface mass (kg/m^2) of the sample, D (N m) the bending stiffness [41],[2] Y(t) is the step function at $t = 0$, Si the sinus integral function: Si(z) $\int_0^z \frac{\sin(t)}{t}dt$.

[2] The bending stiffness can be computed taking the classical lamination theory to take into account the anisotropy of the laminate, or be estimated using an isotropic approximation based on the hypothesis using the main bending mode of the plate. A mean between the x and y directions has been chosen here.

The Green's function is useful to obtain the deflection d(x,y,t,) at point (x,y) and time t for any external applied pressure field P(ξ,η,t) with the convolution product:

$$d(x,y,t) \quad \int d\tau \iint d\xi d\eta G\left(\sqrt{(x\ \ \xi)^2 + (y\ \ \eta)^2}, t\ \ \tau\right)P(\xi,\eta,\tau) \tag{3}$$

At times large with respect to the impact duration, the deflection reaches a constant value called d_∞, which can be obtained from insertion of an asymptotic form of Eq. 2 into Eq. 3.

$$d_\infty \quad \frac{k}{8\sqrt{\mu D}} \tag{4}$$

Where k is the impulse resulting from the integration of the pressure applied on the sample [41,42].

$$k \quad \int d\tau \iint d\xi d\eta\ P(\xi,\eta,\tau) \tag{5}$$

The deflection at large times is extracted from Fig. 9 and the corresponding impulse from Eq. 4. In plane Young moduli and Poisson ratios are obtained from standard laminate theory $E_{xx} = E_{yy} = 50.0$ GPa and $\nu_{xy} = 0.305$. The bending stiffness D (36.4 N/m) is chosen as the mean of the bending stiffness $D_{xx} = 51.8$ N/m and $D_{yy} = 21$ N/m of the composite plate for X (0°) and Y (90°) directions. The thickness h is 2 mm here, and the surface mass is $\mu = 3.1$ kg/m^2.

With this procedure, the applied pressure P(ξ,η,t) and integrated impulse k are indirectly surface state dependent though the usage of the measured deflection from LS tests, although no explicit model of the metallic mesh and paint layer is used. Once the impulse k is known, the Greszczuk theory [42] and the Hertz contact theory [43], are used to identify analytically the mass and velocity of an equivalent impactor. The impulse is thus associated to the momentum *mv*

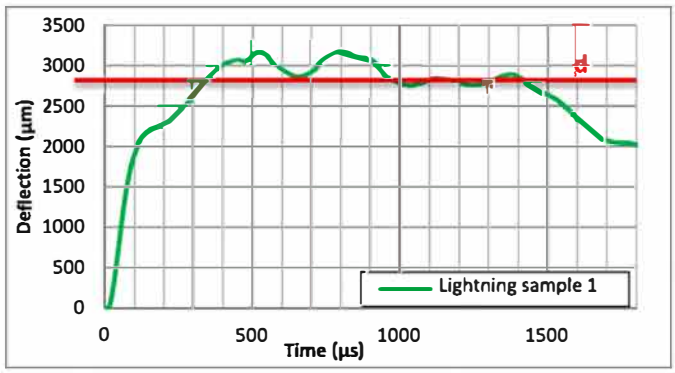

Fig. 9. Displacement vs time curve for lightning sample #1.

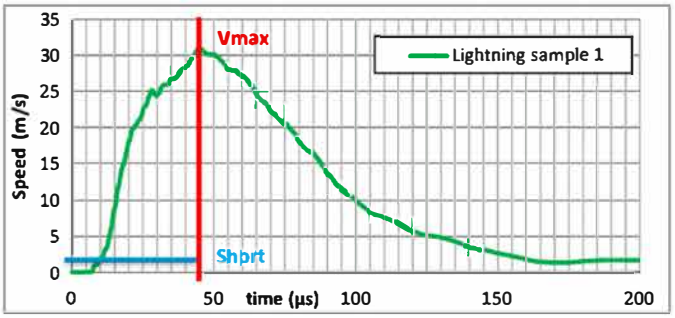

Fig. 10. Velocity vs time curve for lightning sample #1.

of a projectile of mass m, reaching the sample at the speed v, as a consequence of Eq. 3. As a first approximation the maximum speed of deflection measured during lightning strike tests is used as the speed of the projectile (e.g. $v_{max} = 29$ m/s for sample #1). The time duration to this peak value is also extracted as the "short time" which defines the equivalence time for further equivalent mechanical impacts. This duration T is of 47 µs (see Fig. 10). Then, the mass of the associated projectile can be calculated using $k = m.v$. The obtained mass m is of 7.8 g for sample #1. Couples (m, v) associated to each lightning strike are thus obtained. In practice here the radius of the projectile is obtained from its mass using the steel density 7927 kg/m^3.

Table 2 gathers the values of maximum velocity, short time for equivalence and d_∞ for the samples presented in Table 1. It is seen that the greater the rear face velocity of the plate, the greater the value of d_∞.

4. Mechanical tests

The mechanical impact tests are not intended to replicate the surface damage which do not result from a purely mechanical cause, but presumably the depth damage (delamination) occurring in the laminate assuming that similarity of deflections implies similarity of delamination. There are at least two reasons for attempting to use the deflection criterion to define the equivalence between lightning and impacts. The first one is that deflection and velocity are the only quantitative real time data which is actually available from lightning tests. Another criterion which could have been used is the amount of energy available in a mechanical test and in lightning. This has been investigated in [11] and was not successful, the main reason being that only a part of the electrical energy available in the capacitors goes into mechanical damages.

Based on the hypothesis that the deflection criterion can lead to equivalence between lightning and impacts, the process developed in the frame of the paper is the following one: (1) Perform one lightning test where real time deflections and post strike damages are measured, (2) Design impact conditions (m,v) by the analytical approach presented in Section 3, (3) Design and perform mechanical impact tests and numerical model to obtain mechanical deflections and damages, (4) Compare impact deflections and damages to lightning ones, (5) Compare core numerical impact induced damage with damage induced by other equivalent mechanical loadings.

Table 2
Equivalence values for the lightning samples 1 to 4.

Sample #	Vmax (m/s)	Short times (µs)	d_∞ (µm)	K (N.s)	m (g)
1	29	47	2800	0.228	7.8
2	10.6	34	2000	0.16	150
3	57	38	3500	0.285	5
4	83.5	11.5	4400	0.359	4.3

4.1. Specimen manufacturing

Quasi isotropic $[45/0/\ 45/90]_s$ T800/M21 specimens are prepared by hand lay up of unidirectional plies. Samples are square plates of dimensions 400×400 mm^2 and thickness of 2 mm. The samples' curing cycle and polymerization follow standard procedures: 7 bar pressure, 2 h at 180 °C and 0.3 bar Vacuum.

4.2. Canon test set up and instrumentation

Actual canon gas tests were run at the Institut Clément Ader laboratory to validate the results of these impacts predicted by the numerical simulations (Fig. 11.a). Mechanical impact tests were conducted using a stainless steel ball of diameter Φ9.9 mm and mass 4 g as projectile, launched in a range of velocities from 50 to 150 m/s.

The mechanical set up was designed to represent the experimental conditions of the lightning strike tests. Plates are fixed with 12 bolts disposed in a circle of diameter Φ370 mm to reproduce the lightning samples clamping system (Fig. 11.b).High speed cameras are used to measure the projectile velocity at the gas gun exit. Rear face displacements are measured using two displacement sensors (Keyence 20 kHz without contact), one at the rear face centre and the other 10 cm below. Finally, three force sensors are placed between the metallic ring and the assembly to register the total impact force.

4.3. Samples and impact conditions

The canon apparatus allows ejecting the projectile at several velocities depending on the pressure applied in the tube. For practical reasons, the impactor mass is always 4 g. Table 3 provides the different corrected velocities and the actual speed measured by the high speed camera for each sample. Differences are inherent to the experimental apparatus and concordant with the repeatability and the dispersion of the test set up, as observed on similar test campaigns. Reference lightning samples presented in Table 3 have been chosen among several lightning campaigns led by AGI during the past years and selected among several tens of lightning samples. The same type of protection has also been selected for the entire samples: ECF195. Finally, two samples with similar thickness of paint layer have been selected: samples 101 and 102. In order to investigate further the influence of the paint parameter, one sample with a lower paint thickness has been added to the plan, sample 103, along with peculiar samples 107 and 110 which possessed the same amount of paint than sample 101 but with a spare zone at the centre.

5. Comparison of results

Two main features can be extracted from the post mortem non destructive analyses. For impacts at velocities greater than 75 m/s rear face splinters can be observed whom size increases with the velocity (Fig. 12). Indentation is visible for impacts superior to 65 m/s. Penetration is also to be noted for the impact case at 124 m/s at the impact point on the sample. The presence of such damage identifies the limits of the MI as the impulse delivery, because of course marked indentation are never observed during lightning strike. Thus, care must be taken in comparisons.

5.1. Rear face displacements versus time

Fig. 13 presents the rear displacement results for each MI test except the higher one at 124 m/s. Indeed, for the test case at 124 m/s the large splinter generated by the impact interfered with the displacement sensor which cannot follow the punctual displacement, thus, the first peak of deflection is not available for this case. Results

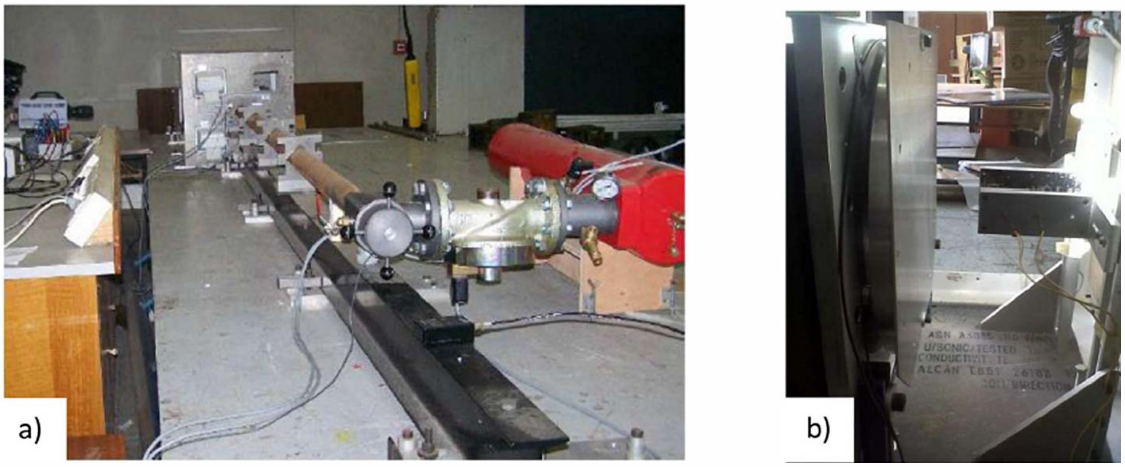

Fig. 11. Mechanical impact setup canon gas gun apparatus (a), (b) circular aluminium clamping ring with sample fastened.

Table 3
Lightning strike cases and their equivalent mechanical impacts.

Lightning strike cases	MI samples	Analytical mass / impulse /velocity	4 g target velocity (m/s)	4 g projectile speed (m/s)
101 (ECF195-P160)	MI4	2.2 g–0.16 N.s–72 m/s	72	75
	MI2			75
	MI7			70
102 (ECF195-P200)	MI1	2 g–0.24 N.s–120 m/s	130	124
103 (ECF195-P50)	MI6	4 g–0.2 N.s–50 m/s	65	50
	MI3			65
107 (ECF195-P160, Φ6mm paint spare)	MI8	2.7 g–0.19 N.s–70 m/s	81	81
110(ECF195-P160, φ12 mm paint spare)	MI5	2.3 g–0.18 N.s–79 m/s	87.5	87.5

for the two tests at 75 m/s show some differences. It should be noted that 75 m/s is an approximate value of the real velocity which was more about 72 m/s for case 2 with a delay in the record for the very first instants while it was more about 77 m/s for case 1. The gap between those two tests is then of the order of 5 m/s. As expected, it can be seen that the higher the projectile velocity, the higher the first deflection peaks. The natural vibration of the plate over time is clearly visible at large times with the particular shape of the first peak due to the impact of the projectile. It is presumed that all dam ages due to the impact appear during this first deflection peak and that the natural vibration of the plate beyond 100 μs does not dam age the sample anymore.

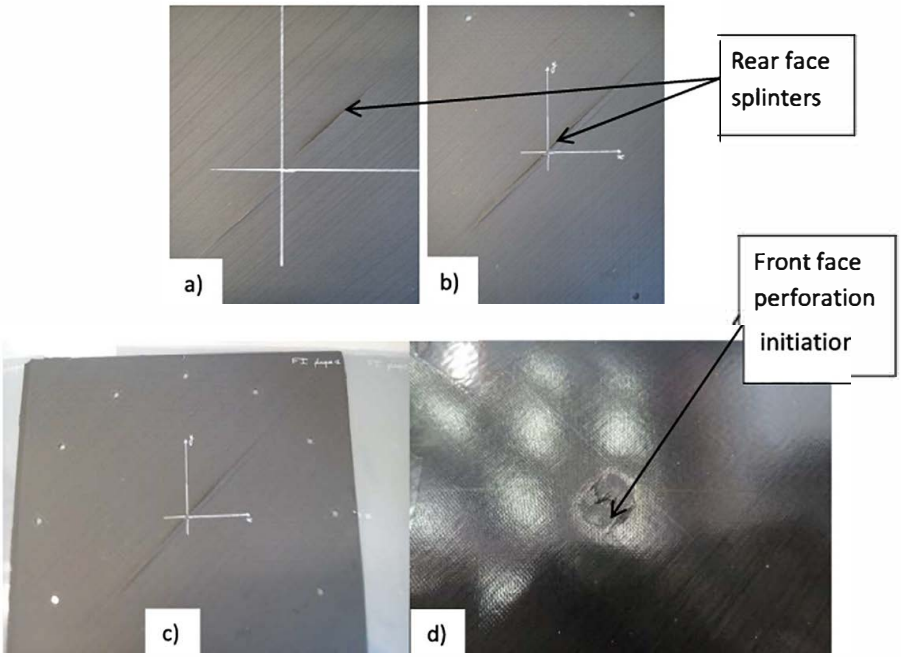

Fig. 12. Observable damage on MI samples (a–b) rear face impact at 80 m/s, (c) rear or (d) front faces impact at 124 m/s.

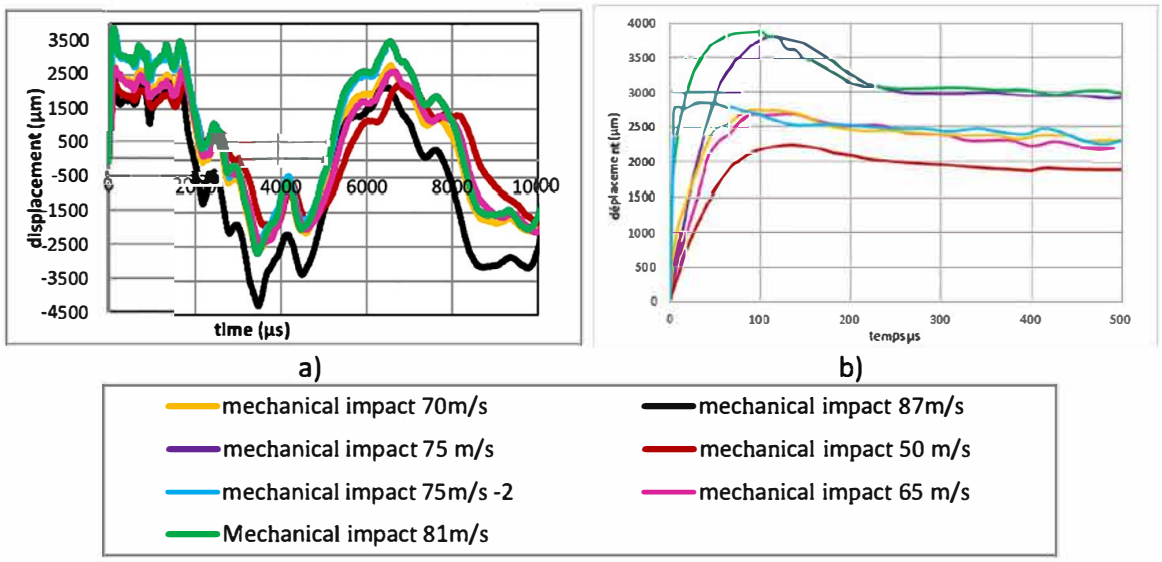

Fig. 13. Rear face displacement results (a) long time results for all tests (b) short time results (zoom between 0 to 500 µs).

From Fig. 13, the different characteristic times are derived. 100 µs is obtained as the mean value for the short times of all experiments. 500 µs is obtained to be the large time, and d_∞ can be obtained from the plateau values on each experimental curve. As the equivalence is made on a short time range (<100 µs) a focus on this period and on the first peak deflection followed by the displacement plateau is made in Fig. 13. As for the force, the maximum deflection increases with impact velocity. For all cases, this maximum value is included in the range {2 mm, 4 mm}.

Table 4 summarizes comparisons of displacements and velocities (slopes of displacements) between LS tests and the corresponding MI ones for the "strike time" (about 50 µs, where maximum value of the velocity is reached for 80 to 87 m/s velocity). A good correlation can be observed, except for cases 2, 3 and 6 due to sensor acquisition problem. The velocity in case 110 is not correctly approximated because the lightning case was particular. Indeed, the paint was not burned thus confining the gas and the melt copper mesh.

A focus on cases 101 and 103 is presented on Figs. 14 and 15 respectively for impacts at 65 m/s, and 75 m/s. For lightning sample 103, which is totally covered by paint, the slope and values of displacement up to 50 µs ('short times') are quite close. Between 50 µs to 100 µs ('Strike times'), displacements are still of the same order of magnitude (about 2.5 mm), and both slopes change with different amplitudes (different decelerations). After 100 µs ('Stabilization times'), the two curves separate. The mechanical impact curve tends to decrease. The lightning strike displacement increases further.

For lightning sample 101, the lightning curve is surrounded by the two MI tests at 70 m/s and 75 m/s. The impact tests at 75 m/s better reproduced the slope of displacement of LS; however, its maximum displacement seems to be a bit too high.

The difference of displacements between samples 101 and 103 (Fig. 16) is due to differences in surface states. Remember that in the LS test 101, the paint was burned but not removed from the top layers. Sample 101, with 160 µm paint clearly shows a larger delaminated area as well as a higher displacement peak. The perturbation due to the paint also explains this strong difference: in the lightning strike test 101, the paint is burned on a very small part at the root attachment and so disturbs very soon and all the LS test long the global behaviour of the plate. For sample 103 on the contrary the lighter paint thickness was completely burnt so that the paint did not disturb for a long time the plate behaviour.

5.2. Delaminated surfaces

The total damaged area in the samples is obtained summing the projected views of the damage in each interface from C Scan measurements (ellipsoid contouring). Measures using C Scan are done from the two faces of the laminates when it's possible (no important damages on the rear face of the plate). By doubling the post mortem scanning on MI samples, it is possible to confirm also the number, size and position of each delamination but also to reveal smaller ones that would be hidden by bigger ones. Each delamination is defined by its position in the laminate, which is identified by the corresponding colour in the colour map of the C Scan measures. The variability of the area is about 10%. For LS tests, measures are done from the rear face only because of the metallic mesh disturbance in the impacted face. Indeed, some delamination could be hidden by big surfaces in LS tests.

Table 5 presents the total delaminated area measured for each LS test and its associated MI test, and the relative difference. It can be

Table 4
Displacements and velocities at 50 µs.

Lightning samples	LS displacement (µm)	Mech. Impact displ. (µm)	Relative difference	LS velocity (m/s)	Mech. Impact vel. (m/s)	Relative difference
101	2839	(4) 2850	0.8%	37.4	33.6	−10.1%
		(2) 2843	0.5%		22.9	−37.8%
		(7) 2560	−9.4%		35.3	−5.8%
103	1810	(6) 2153	+18.9%	25.9/30	33.8	+32%
		(3) 1863	+2.9%		31.2	+21.8%
107	2626	(8) 3630	+38.2%	32.3	27.3	+9.6%
110	2605	(5) 2486	−4.6%	37.2	15.2	−59.1%

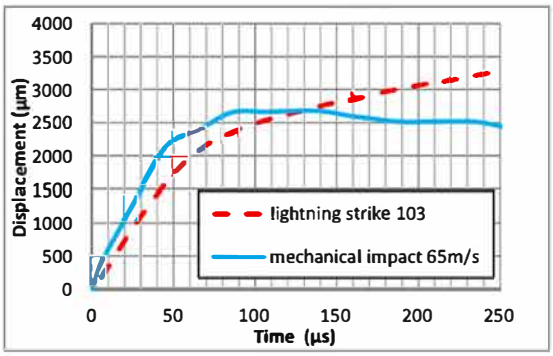

Fig. 14. Displacement versus time for the 65 m/s MI test (full line) and LS case 103 (dashed line).

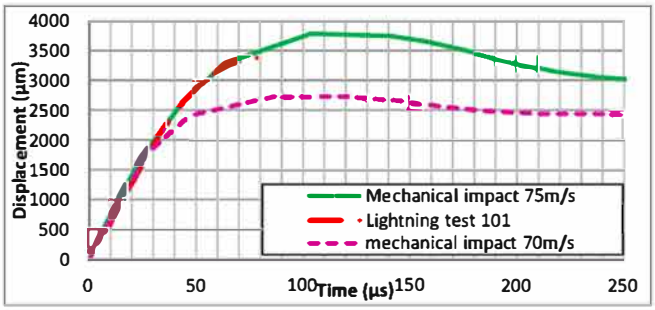

Fig. 15. Displacement versus time for the 70 m/s and 75 m/s mechanical impact tests and lightning strike cases 101.

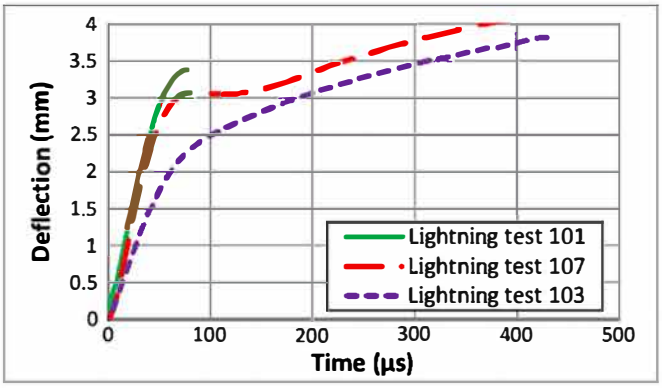

Fig. 16. Comparison of displacement for LS tests 101 and 107 (ECF195-160 µm paint).

noticed that the delaminated surfaces in cases 101 are higher in LS than in mechanical impacts due to paint influence. Some observations are made on the parameter 'paint thicknesses'.

Remember that for sample 101 the paint was not removed by the lightning strike while for sample 107 the central zone was unpainted on a spot zone of a few 6 mm in diameter so that its effect is delayed in time. The delaminated area is bigger in the case 101 in spite of the same thickness of paint for the two lightning samples. This difference is attributed to the spare paint area on sample 107 which delays the confining effect of paint and provides protection with respect to the arc attachment. We can notice on Table 5, there is no delamination for case 103 lightning sample while for MI3 and MI6 samples delaminated areas measure 223 mm^2 and 630 mm^2. Delaminated areas are located in the top interfaces and are due to the contact by the projectile, illustrating the limit of the comparison methodology for low velocities.

Fig. 17 presents the evolution of the total delaminated area as a function of the projectile's velocity for MI tests and the maximal plate speed for LS tests. As expected, the higher the projectile's velocity, the higher the damage area for both LS and MI tests. The curve can be approximated by a linear function of slope 81 mm.ms ($R = 0.94$) or by a cubic curve which is more compatible with the limit of the contact impact approximation which creates large cracks in the rear face. The cubic approximation gives the delaminated area y as a function of the projectile velocity x with a regression coefficient of 0.98: $y = 0.04x^3 + 11.3x^2$ 854x + 20,097. It can be seen that LS and MI curves are quite close, even for the high speed case at 124 m/s which was not good for rear face analyses. This again proves the validity of the model of equivalent impulse.

5.3. *LS versus MI delamination distribution*

Fig. 18 presents histograms of the size and position of the main delamination measured from C Scans through the laminate thickness for both MI tests and LS cases 101 and 107. The position zero corresponds to the rear face of the laminate, opposite to the impacted side. Histograms clearly show the difference in delamination position through the thickness for the two kinds of impacts.

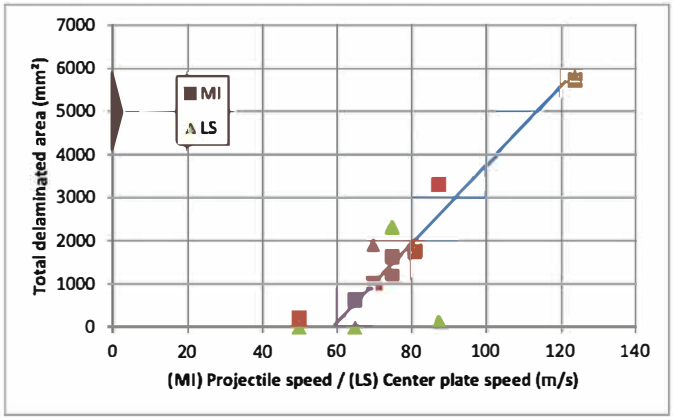

Fig. 17. Total delaminated area as a function of the velocity.

Table 5
Delaminated area for lightning strikes and associated mechanical impacts.

Lightning samples	Associated mechanical samples	Projectile's speed (m/s)	LS delaminated area (mm^2)	Mechanical delaminated area (mm^2)	Relative difference
101	MI4	75	1900to 2320	1626	−29%
	MI2	75		1184	−49%
	MI7	70		1019	−56%
102	MI1	124	5836	5732	−2%
103	MI6	50	0	223	–
	MI3	65		630	–
107	MI8	81	1737	1746	−2%
110	MI5	87.5	120	3361	–

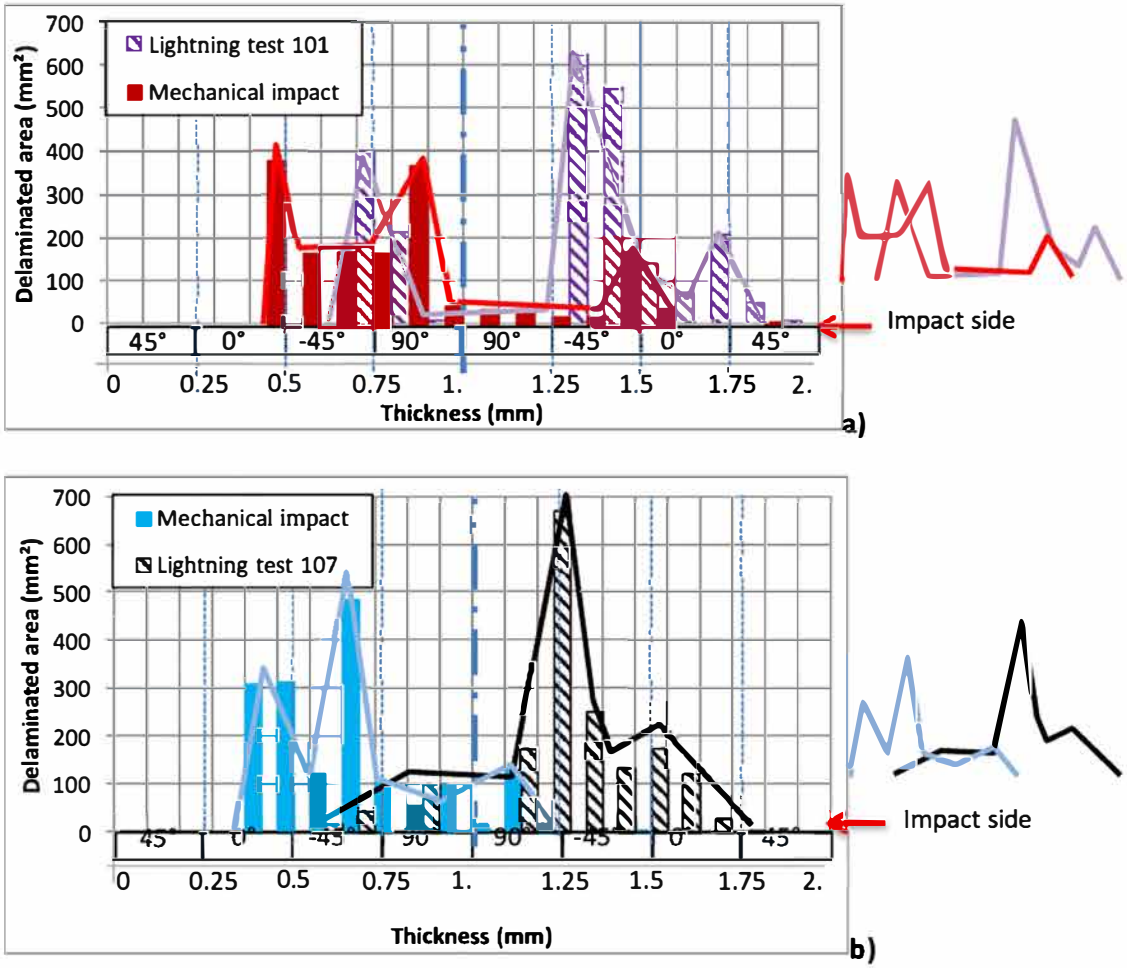

Fig. 18. Histograms of the delamination as a function of position in the thickness (as defined in fig. 6) of the material, for # 101 (a) and # 107 (b) samples.

Damage is essentially concentrated in the first half thickness close to the stroke side for LS tests while MIs larger damage are located in the second half thickness closer to the rear face.

Profiles extracted from the maximal values (**envelope**) highlight a great difference that is not yet completely explained, and could come from effects not taken into account here, in particular the impulse delivery surface which is a point for a sphere impact but evolves rapidly during the very rapid burning progress of the LSP layers up to a disk of about 12 mm diameter. This idea comes from analyses on geometric transformations both in abscissa and in ordi nate of the envelope of the delamination profiles (Fig. 18), that are applied on the MI tests curves to fit the first delaminated peak (abscissa translation) and to the maximal delaminated area (scale factor on ordinate, second peak in LS tests). No scale factor is applied on abscissa. The result can be observed on Fig. 19. The offset between curves represents indeed the offset of delamination in dif ferent interfaces. The offset of delamination location is suspected to be due to the difference of loading rates between MI and LS that locates the peak stress responsible of the delamination onset at dif ferent positions in the depth. This phenomenon is described by Ecault et al. [19] who control the laser impulse to enforce the onset of delamination in a chosen interface.

For case 101, the MI tendency curve is delayed from of 0.25 mm in abscissa which coincides with one ply thickness, and scaled in ordinate by a factor of 1.55 to fit the maximum delaminated area of the LS test. A distance of about one ply in thickness (0.25 mm) can still be observed between the two second peaks from impact side. A similar third peak is observed in rear interfaces in both cases (Fig. 18). This allows thinking that the loading rate and amplitude were higher in the LS than in the MI test and that delamination in higher interfaces in LS tests are due to this. Remembering that the paint was not burned in this test, we conclude that the paint removal

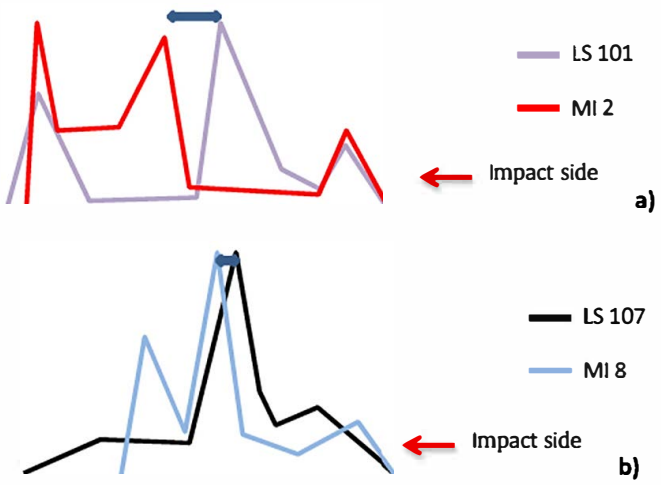

Fig. 19. Comparison of MI versus LS delamination profiles for cases 101 (a) and 107 (b).

has probably an effect in the very beginning of the lightning process and that the main delamination is created in less than 50 μs.

For case 107, the first delaminated interface in MI test is moved two plies deeper in the thickness (0.5 mm) to fit the LS test one, and a scale factor of 1.31 is applied to the ordinate of the MI tendency curve to fit the maximal value of the second peak. For this case, there is no delay in the two peaks between LS tests and MI tests. Remem bering that the centre of the composite plate is not paint, it is con cluded again that the paint has an effect on the rate and the amplitude of the load delivery which are related to both the extent and the location in depth of the delamination. It is concluded that the paint surface that is active is about a radius from 3 mm to 6 mm.

6. Conclusion

The main objective of this paper was to propose an analytical method to design mechanical experimental tests that are simpler while representative of complex lightning tests, and evaluate the validity of the design for protected and painted composite panel. The model that is proposed here uses the two main hypotheses that surface and core damage observable on post mortem stroke samples can be separated, and that the complex events that arise in the lightning strike protection layers (paint plus metallic mesh) can be replaced by a purely mechanical impulse delivery on the bare composite.

Comparisons of the rear face displacements show that our analyt ical method is able to reproduce most of the LS reference cases, pro viding that the velocity of the rigid sphere for the MIs is high enough to touch properly the sample and low enough to avoid too large indentation of the impacted face and splinters in the rear face. This result proves that the analytical equivalent impulse model is valid, and thus the two main hypotheses also.

By pushing forward the analysis, the damage total surface and distribution through thickness of the composite panels have been compared. It is shown that total delaminated surfaces are quite close and follow the same evolution with increasing impulse. Impulse depends for LS only on the protection layers' characteristics. One important result is nevertheless a poor correspondence between the delamination distribution between LS and MI tests. It is shown that delamination induced by LS are mainly localised into the first half on the thickness while they are localised in the second for MI tests. This discrepancy highlights the need to investigate more precisely how the impulse is delivered both in time and space in LS and MI. In par ticular, it highlights the need to investigate further the particular effect of the paint burning and erosion resistance. This point will be one of the main efforts of coming work.

Acknowledgements

DGA Ta is gratefully thanked for the tests results used in this study. All technical staffs of ISAE SUPAERO, ICA, and AGI are grate fully thanked for their help or collaboration.

References

[1] Deeg EW. New algorithms for calculating hertzian stresses, deformations, and contact zone parameters. AMP J Technol 1992;2:14–24 1992.
[2] Rupke E. Lightning direct effects handbook, lightning technologies inc. Rept. AGATE-WP3.1-031027-043, Pittsfield, MA, 1 March.
[3] Fisher FA, Plumer JA. Aircraft lightning protection handbook. Lightning Technologies; 1989 Inc., Rept. FAA/CT-89/22.
[4] Perrin E. Modélisation des effets indirects de la foudre sur avion composite PhD Thesis of the Université de Limoges. 2010; 192.
[5] Chen J, Allahdadi F, Carney T. High velocity impact of graphite/epoxy composite laminates. Compos Sci Technol 1997;57(9/10):1369–79.
[6] Hirano Y, Katsumata S, Iwahori Y, Todoroki A. Artificial lightning testing on graphite/epoxy composite laminate. Composites Part A: Applied Science and Manufacturing, 41; 2010. p. 1461–70. doi: 10.1016/j.compositesa.2010.06.008.
[7] Ogasawara T, Hirano Y, Yoshimura A. Coupled thermal-electrical analysis for carbon/epoxy composites exposed to simulated lightning current. Composite Part A: Applied Science and Manufacturing, 41; 2010. p. 973–81. doi: 10.1016/j.compositesa.2010.04.001.
[8] Gagné M, Therriault D. Lightning strike protection of composites. Prog Aerosp Sci 2014;64:1–16. doi: 10.1016/j.paerosci.2013.07.002.
[9] Gou J, Tang Y, Liang F, Zhao Z, Firsich D, Fielding J. Carbon nanofiber paper for lightning strike protection of composite materials. Composites Part B: Engineering, 41; 2010. p. 192–8. doi: 10.1016/j.compositesb.2009.06.009.
[10] Duong Q, Guo Y, Sun X, Jia Y. Coupled electrical-thermal-pyrolytic analysis of carbon fiber/epoxy composites subjected to lightning strike. Polymer 2015;56 (15):385–94. doi: 10.1016/j.polymer.2014.11.029.
[11] Lepetit B, Soulas F, Guinard S, Revel I, Peres G, Duval Y. Analysis of composite panel damages due to a lightning strike: mechanical effects. In: International Conference on Lightning Static Electricity (ICOLSE); 2013.
[12] Lago F. Measurements by stereo correlation of the deflection of panels submitted to lightning pulse currents. In: International Conference on Lightning and Static Electricity (ICOLSE); 2011.
[13] Ackermann PK. Paint thickness comparison over composite lightning surface protection systems and in-service ramifications. In: International Conference on Lightning and Static Electricity (ICOLSE) 2005; 2005.
[14] Mc Keeman Brown A. Evaluating surface protection systems for aerospace composites. In: International Conference on Lightning and Static Electricity (ICOLSE); 2005.
[15] Lightning. Internal report performed by Airbus Group Innovations. 32064-1-IW-SP.
[16] Li Y, Li R, Lu L, Huang X. Experimental study of damage characteristics of carbon woven fabric/epoxy laminates subjected to lightning strike. Composites Part A: Applied Science and Manufacturing, 79; 2015. p. 164–75. doi: 10.1016/j.compositesa.2015.09.019.
[17] Feraboli P, Kawakami H. Damage of carbon/epoxy composite plates subjected to mechanical impact and simulated lightning. J Aircr 2010;47(3):999–1012. doi: 10.2514/1.46486 2010.
[18] Michel Y, Le Roux N, Durin C, Espinosa C, Moussi A, Chevalier JM, et al. Damages and matter ejection during HVI on brittle structures: implications for space environment. In: 10th Symposium on Materials in Space Environment; 2006.
[19] Ecault R, Boustie M, Touchard F, Pons F, Berthe L, Chocinski-Arnault L, et al. A study of composite material damage induced by laser shock waves. Compos Part A 2013;53:54–64. doi: 10.1016/j.compositesa.2013.05.015.
[20] Chemartin L, Lalande P, Peyrou B, Chazottes A, Elias PQ. Direct effects of lightning on aircraft structure: analysis of the thermal, electrical and mechanical constraints. J Aerosp Lab 2012;5(AL05-09):1–15 2012.
[21] Lago F, Gonzalez JJ, Freton P, Uhlig F, Lucius N. A numerical modelling of an electric arc and its interaction with the anode: part III. Application to the interaction of a lightning strike and an aircraft in flight. J Phys D: Appl Phys 2006;39:2294–310. doi: 10.1088/0022-3727/39/10/045.
[22] Tholin F, Chemartin L, Lalande P. Numerical investigation of the interaction of a lightning and an aeronautic skin during the pulsed arc phase. In: International conference on lightning and static electricity (ICOLSE); 2015.
[23] Feraboli P. Some recommendations for the characterization of the impact performance of composite panels by means of drop tower impact testing. J Aircr 2006;43(6):1710–8. doi: 10.2514/1.19251 2006.
[24] Feraboli P, Kedward KT. Enhanced evaluation of the low velocity impact response of composite plates. AIAA J 2004;42(10):2143–52. doi: 10.2514/1.4534 2004.
[25] Kan HP. Enhanced reliability prediction methodology for impact damaged composite structures, U.S. Dept. of Transportation, Rept. DOT/FAA/AR-97/79. 1998.
[26] Gineste PN, Clerc R, Castanié C, Andreu H, Buzaud E. Assessment of lightning direct effects damages by modelling techniques. In: Int. Aerospace and Ground Conf. on Lightning and Static Electricity 2009; 2009.
[27] Featherston CA, Eaton MJ, Evans SL, Holford KM, Pullin R, Cole M. Development of a methodology to assess mechanical impulse effects resulting from lightning attachment to lightweight aircraft structures. Appl Mech Mater 2010;24–25: 129–34. doi: 10.4028/www.scientific.net/AMM.24-25.129.
[28] Heidlebaugh D, Avery W, Uhrich S. Effect of lightning currents on structural performance of composite materials. In: International Conference on Lightning and Static Electricity (ICOLSE); 2001.
[29] Feraboli P, Miller M. Damage resistance and tolerance of carbon/epoxy composite coupons subjected to simulated lightning strike. Composites Part A: Applied Science and Manufacturing 2009, 40; 2009. p. 954–67. doi: 10.1016/j.compositesa.2009.04.025.
[30] Wang FS, Ding N, Liu ZQ, Ji YY, Yue ZF. Ablation damage characteristic and residual strength prediction of carbon fiber/epoxy composite suffered from lightning strike. Compos Struct 2014;117:222–33. doi: 10.1016/j.compstruct.2014.06.029.
[31] Wang Y, Zhupanska OI. Lightning strike thermal damage model for glass fiber reinforced polymer matrix composites and its application to wind turbine blades. Compos Struct 2015;132(15):1182–91. doi: 10.1016/j.compstruct.2015.07.027.
[32] Lepetit B, Escure C, Guinard S, Revel I, Peres G, Duval Y. Thermo-mechanical effects induced by lightning on carbon fibre composite materials. In: International Conference on Lightning and Static Electricity (ICOLSE); 2011.
[33] Abdelal G, Murphy A. Nonlinear numerical modelling of lightning strike effect on composite panels with temperature dependent material properties. Compos Struct 2014;109:268–78. doi: 10.1016/j.compstruct.2013.11.007.

[34] Haigh SJ. Impulse Effects during Simulated Lightning Attachments to Lightweight Composite Panels. In: International Conference on Lightning and Static Electricity (ICOLSE); 2007.
[35] Karch C, Honke R, Steinwandel J, Dittrich KW. Contribution of lightning current pulses to mechanical damage of CFRP structures. In: International Conference on Lightning and Static Electricity (ICOLSE); 2015.
[36] Liu ZQ, Yue ZF, Wang FS, Ji YY. Combining analysis of coupled electrical-thermal and blow-off impulse effects on composite laminate induced by lightning strike. Appl Compos Mater 2015;22(2):189–207. doi: 10.1007/s10443-014-9401-8.
[37] Wang FS, Ding N, Liu ZQ, Ji YY, Yue ZF. Ablation damage characteristic and residual strength prediction of carbon fiber/epoxy composite suffered from lightning strike. Compos Struct 2014;117:222–33. doi: 10.1016/j.compstruct.2014.06.029.
[38] Guinard S., Analyse de la tenue aux impacts à faible énergie et faible vitesse des structures en stratifié composite. Thèse de doctorat de l'Ecole Normale Supérieure de Cachan. Université Paris 6, 2001, 124 p.
[39] EUROCAE ED-84, Aircraft Lightning Environment and Related Test Waveform Standard, 1997.
[40] SAE Committee report: ARP-5412, Aircraft Lightning Environment and Related Test Waveforms Standard, 1999.
[41] Filippi PJT. Vibrations et vibro-acoustique des structures minces. Hermès Sciences Publications; 2008 ISBN-10: 2746219379. ISBN-13: 978-2746219373.
[42] Greszczuk. Damage in composite panels due to low velocity impact. In: Zukas ZA, editor. Impact dynamics. Wiley; 1982. p. 55–94.
[43] Soulas F. Development of a lightning strike mechanical model for the prediction of damage of aeronautical composite panels PhD Thesis Université de Toulouse. 2016242.